SPE Brazil Flow Assurance Technology Congress
Rio de Janeiro, Brazil, November 15 – 18 2022

Features of the liquid film in vertical downward annular flow

Ana Luiza B. Santana[1*], Eduardo N. dos Santos[1], Marco J. da Silva[1], Moisés A. Marcelino Neto[1], Rigoberto E. M. Morales [1]
[1]Multiphase Flow Research Center (NUEM), Federal University of Technology – Paraná (UTFPR), Brazil
[*]anasantana@alunos.utfpr.edu.br

Abstract
This work performed experiments to characterize the liquid film in vertical downward air-water annular flow in a 26-m ID, 14-m long pipe. A non-intrusive dual ring-shaped conductance sensor and an intrusive capacitive with a 16 x 16 wire-mesh sensor (WMS) arrangement were deployed in the test section and placed at 335D from the flow inlet to measure temporal and spatial information about the liquid film. Thirty-five flow conditions with superficial air and water velocities ranging from 0 m/s to 20 m/s and 0.05 m/s to 0.25 m/s, respectively, were investigated. Time-series analyses provided film features such as the average liquid thickness and disturbance wave properties such as velocity, frequency, amplitude, and length. Flow reconstructions were made to corroborate the liquid film analyses from the WMS measurements. Droplets that flow along with the gas phase in the core of the flow were also identified.

Keywords
Liquid film; conductance sensor; wire-mesh sensor

Introduction
The annular two-phase flow is characterized by a continuous, fast-moving gas core laden with droplets and a liquid film wetting the pipe wall. This flow pattern is often observed in pieces of industrial equipment such as nuclear reactor systems, evaporators, condensers, and the oil and gas industry, notably in gas wells with condensate [1].
The gas-liquid interface of the annular flow is irregular because of the presence of waves, structures named in the literature as disturbance waves and ripples, as illustrated in Figure 1. The remaining portion of the liquid film is identified as substrate or base film. The waves are formed due to the action of inertia, the gravitational force, and the gas shearing on the interface. Moreover, the gas-liquid interface in vertical downward annular flow (VDAF) is circumferentially non-uniform regarding wave activity. The shape of the interface would depend on the phase flow rates and, in some works, it was associated with the roughness in single-phase turbulent pipe flows to determine the interfacial shear stress [2]. Furthermore, it has been observed that the disturbance waves caused liquid entrainment into the core flow because of the interaction between the liquid and the gas phases. The liquid entrainment affects the interfacial shear friction that influences the pressure drop and the two-phase transfer of momentum, mass, and heat [3]–[5]. In addition, the disturbance waves are inertia-dominated structures that travel along with the liquid film at more significant velocities than those of the substrate, and ripples can be observed on the surface of the disturbance waves. The aim of this article is to provide an experimental characterization of the liquid film to complement the information in the literature, optimize models [6], [7], and contribute to the enhancement of the monitoring processes that guarantee flow assurance in the oil and gas industry.

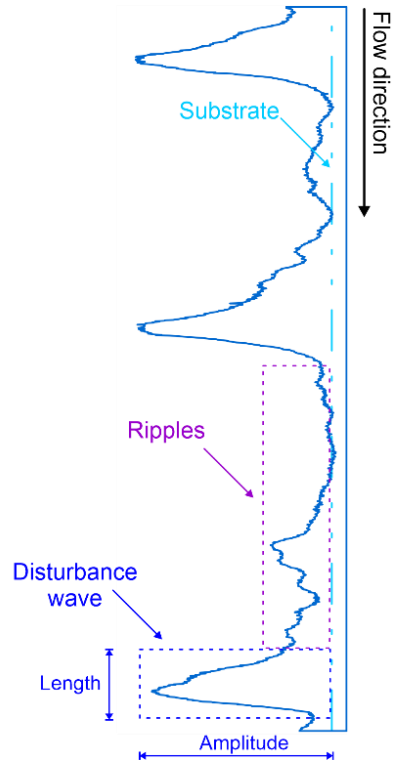

Figure 1 – Representation of the liquid film in an annular flow pattern.

Methodology

The experiments were conducted in the Multilab facility at the Multiphase Flow Research Center (NUEM) of the Federal University of Technology – Paraná (UTFPR). An apparatus was designed to carry out measurements in vertical downward annular flow. The rig has a 26-mm ID and 14-m long test section made of transparent Plexiglas, as shown in Figure 2 – Schematic of the experimental apparatus (D=26 mm). The flow is analyzed in the test section placed at 335D from the flow inlet, where a non-intrusive dual ring-shaped conductance sensor (CS) and an intrusive capacitive 16 x 16 wire-mesh sensor (WMS) were deployed. The sensors can retrieve important information from the liquid film and its distribution. The data acquisition frequencies were 10 kHz and 2 kHz for CS and WMS, respectively, with a sampling time of 30 s. Water from a tank is pumped into the circuit line, where a Coriolis flowmeter monitors the liquid mass flow rate, density, and temperature. An empirical correlation was used to obtain the water kinematic viscosity from the temperature [8].

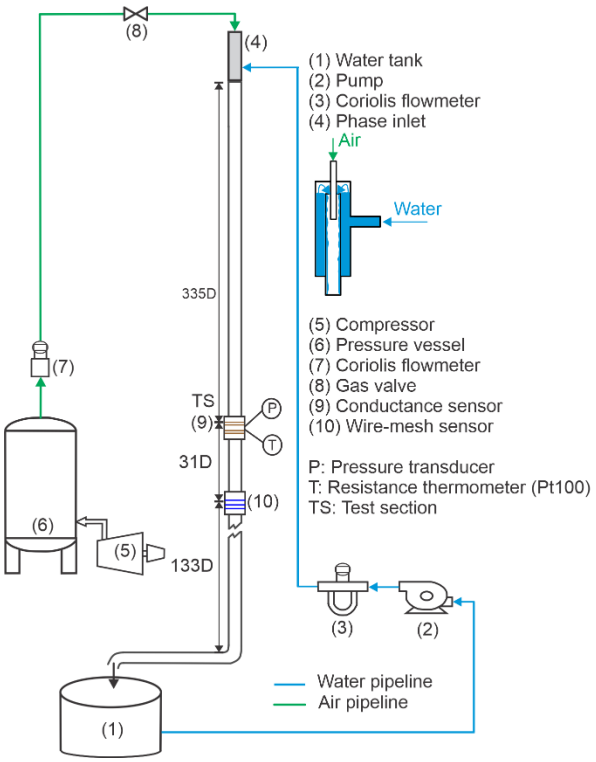

Figure 2 – Schematic of the experimental apparatus (D=26 mm).

An inlet made with concentric pipes was used to inject the phases into the main pipe section. The experimental evaluation comprises thirty-five (35) combinations of gas (J_G) and liquid (J_L) superficial velocities ranging from 0 m/s to 20 m/s and 0.05 m/s to 0.25 m/s, respectively. The flow combinations C01 up to C07 fall into the falling film flow pattern (J_G=0 m/s), while the others fall into the annular flow pattern, as plotted on the flow map proposed by [9] and presented in Figure 3. All phase parameters and data acquisition were controlled, registered, and supervised by supervisory management built as a LabVIEW platform.

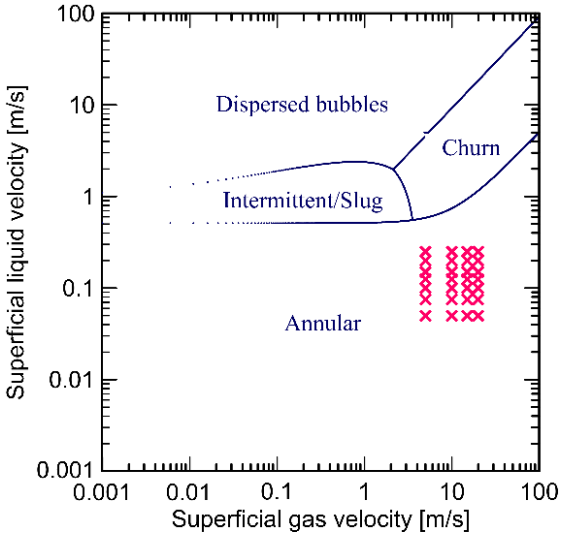

Figure 3 – Experimental combinations of superficial phase velocities plotted on the flow map proposed by [9].

Results and Discussion

This section presents the main results obtained and whose aim is to characterize the liquid film in vertical downward air-water annular flows. Initially, the features of the liquid film will be quantitatively analyzed. Then, a droplet identification in the gas core will be presented. The liquid film features are acquired by processing the time signal measurements obtained by the conductance sensor. The average liquid thickness is determined by the mean of the liquid film's time signal. The disturbance wave (DW) velocity is calculated by a cross-correlational function between the time signal of each sensor channel (CH1 and CH2). The disturbance wave frequency was determined by direct identification of each DW, then calculated by the ratio between the number of DWs and the sampling time. The droplet's information is obtained by gathering the spatial measurements performed by the wire-mesh sensor.

Figure 4 presents the average liquid thickness, the DW velocity, and the DW frequency as a function of superficial phase velocities. The average liquid thickness has a well-defined trend increasing through the range of superficial liquid velocities while J_G remains constant. Moreover, the opposite effect, a reduction of the liquid thickness, was observed with an increase in the superficial gas velocity. On the other hand, the disturbance wave velocity and frequency tend to increase with both superficial phase velocities.

Comparing the parameters between falling films (J_G=0 m/s) and the annular flow with the superficial gas velocity of J_G=5 m/s, it is possible to observe

that the patterns have a closer behavior. An exception is kept for the DW velocity for annular flow with a superficial liquid velocity greater than J_L=0.125 m/s, which presents a higher value, as shown in Figure 4 (b).

Figure *5* presents the geometrical characteristics of the disturbance waves. It can be observed that the amplitude tends to increase with J_L. Regarding the superficial gas velocity, both geometrical parameters decrease with the increase of J_G. The highest DW amplitude is observed in the annular flow with J_G=5 m/s and J_L=0.25 m/s. It is interesting to observe that the flow rate combinations affect wave activity. The gas-liquid interface interaction provides the variation of the wave amplitude because of the increased inertia and surface tension force

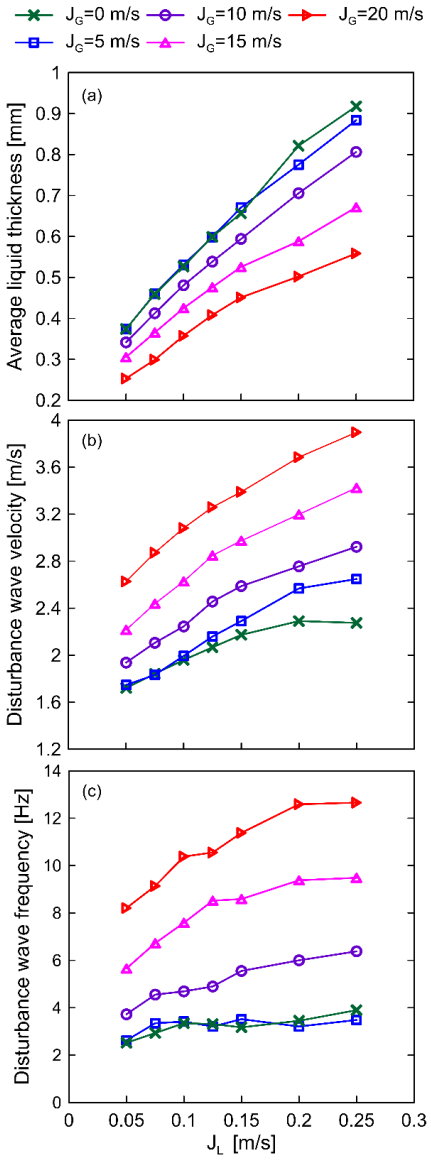

Figure 4 – Results of the liquid film features: (a) average liquid thickness, (b) disturbance wave velocity, and (c) disturbance wave frequency.

Figure 6 shows the median shape of the disturbance wave in the annular flow with J_G=5 and 20 m/s for all the range of superficial liquid velocity.

Comparing the DW amplitude and length, a significant difference is observed. The geometrical characterization of the liquid film waves is used to classify the different wave regimes as proposed by [10].

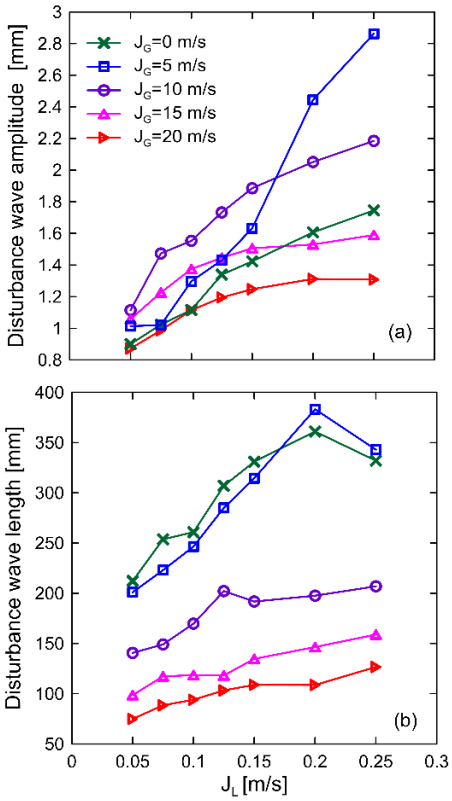

Figure 5 – Geometrical characteristics of disturbance waves: (a) amplitude and (b) length.

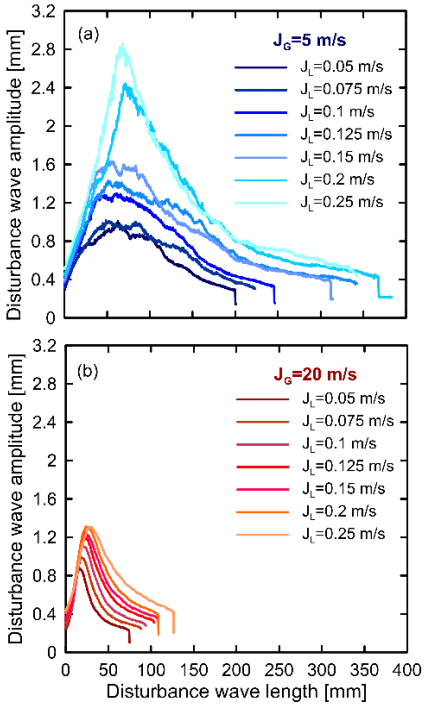

Figure 6 – Median shape of the disturbance waves.

Figure 7 presents the droplets identified for two different combinations of superficial phase velocities, C14 – J_L=0.25 m/s; J_G=5 m/s and C35 – J_L=0.25 m/s; J_G=20 m/s, for all data acquisition time. It can be observed that the superficial phase velocity affects the number, size, and cross-sectional distribution of the droplets in the pipe.

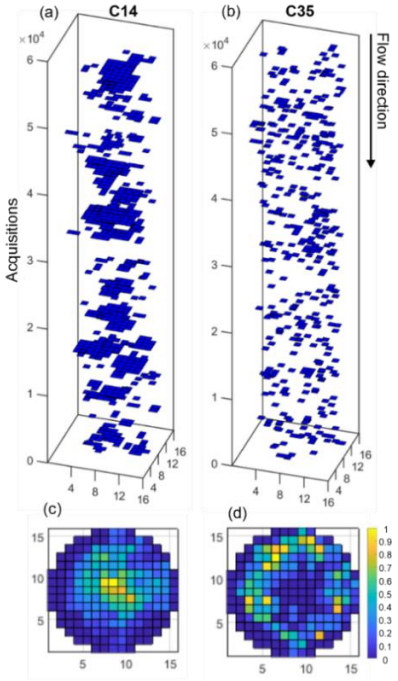

Figure 7 – (a)-(b) Droplets identified in the gas core. (c)-(d) Distribution of the droplets identified in the cross-sectional of the pipe.

The number of droplets identified in the core of gas as a function of superficial phase velocity is shown in Figure 8. Droplets are identified for all 35 flow conditions investigated in this work, and the number of droplets increases with J_L and J_G. An exception is observed for the flow condition with the maximum superficial gas velocity that tends to stabilize for J_L=0.125 m/s. This behavior is due to the small size of the droplets in these annular flow conditions, rendering the measurement difficult.

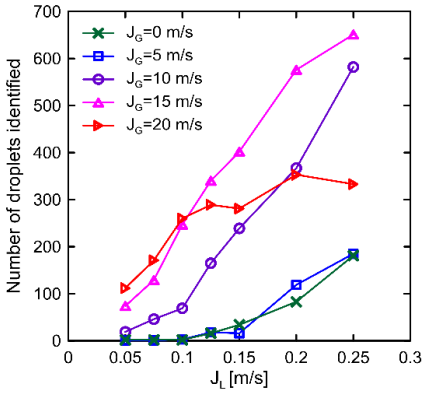

Figure 8 – Number of droplets identified.

Conclusions

This work presents the experimental characterization of the liquid film in downward vertical air-water annular flows in a 26-mm ID, 14-m long pipe. The experimental results evaluated the liquid film features, and further analyses will be shown in the full paper version.

Acknowledgments

The authors would like to express their gratitude for the financial support given by PETROBRAS/CEPES.

Responsibility Notice

The authors are the only ones responsible for the paper contents and opinions expressed in this article.

References

[1] N. S. Hewitt, G F and Hall-Taylor, *Annular Two-Phase Flow*. Oxford: Pergamon Press, 1970.

[2] R. J. Belt, J. M. C. Van't Westende, and L. M. Portela, "Prediction of the interfacial shear-stress in vertical annular flow," *International Journal of Multiphase Flow*, vol. 35, no. 7, pp. 689–697, 2009, doi: 10.1016/j.ijmultiphaseflow.2008.12.003.

[3] G. B. Wallis, "Annular Two-Phase Flow Part 1 : A Simple Theory," no. 25, pp. 59–72, 1970.

[4] M. Ishii and M. A. Grolmes, "Inception Criteria for Droplet Entrainment in Two Phase Concurrent Film Flow," vol. 21, no. (MARCH, 1975), 1975.

[5] B. J. Azzopardi, "Drops in annular two-phase flow," *Int. J. Multiphase Flow*, vol. 23, no. 97, pp. 1–53, 1997.

[6] I. N. Alves, E. F. Caetano, K. Minami, and O. Shoham, "Modeling Annular Flow Behavior for Gas Wells," 1991.

[7] J.-M. le Corre, "Phenomenological model of disturbance waves in annular two-phase flow," *International Journal of Multiphase Flow*, vol. 151, p. 104057, Jun. 2022, doi: 10.1016/j.ijmultiphaseflow.2022.104057.

[8] P. J. Pritchard, *Fox and McDonald's Introduction to Fluid Mechanics*, 8th ed. Hoboken, NJ: John Wiley & Sons, Inc, 2011.

[9] Yehuda. Barnea, Dvora; Shoham, Ovadia and Taitel, "Flow Pattern Transition for Vertical Downward Two-Phase Flow," 1982.

[10] I. Zadrazil, O. K. Matar, and C. N. Markides, "An experimental characterization of downwards gas-liquid annular flow by laser-induced fluorescence: Flow regimes and film statistics," *International Journal of Multiphase Flow*, vol. 60, pp. 87–102, 2014, doi: 10.1016/j.ijmultiphaseflow.2013.11.008.